DOI: 10.1002/adma.200600491

Conjugated Polymer Nanoparticles via Intramolecular Crosslinking of Dendrimeric Precursors**

By *Prasad Taranekar, Jin-Young Park, Derek Patton, Timothy Fulghum, Glenn J. Ramon*, and *Rigoberto Advincula**

π-Conjugated electro-optically active dendrimers are of current interest for developing efficient electroluminescent display devices and other photonic applications.[1] They have unusual electronic and photophysical properties, for example, intramolecular energy transfer in multichromophoric systems, exciton and charge localization phenomena, and photovoltaic effects have been observed.[2,3] A number of these conjugated polymer dendrimer systems are based on poly(phenylene ethynelenes),[4] polyphenylenes,[5] polythiophenes,[5,6] etc. Conjugated polymers based on the carbazole unit are of interest because of their role in electrochromic devices, electrochemical transistors, microcavity photoconduction, electroxerography, and as photovoltaic components that can provide a very efficient matrix for current carrier transport.[7] Polycarbazole and carbazole containing dendrimers that show efficient hole-transport properties and nonlinear optical properties have also been reported.[8]

Intramolecular crosslinking of nano-objects after assembly has emerged as a viable strategy for imparting robustness created by intramolecular crosslinking. This allows expansion of applications for these objects as synthetic antibodies,[9] core crosslinked nanoparticles,[10] shell crosslinked nanoparticles,[11a,b] and shell crosslinked rods.[11c] An advantage is their environmental stability, i.e., both chemical and physical, compared to their noncrosslinked precursors. Chemical or physical crosslinking of dendrimers has attracted a lot of attention recently with focus on both inter- and intramolecular crosslinking.[12,13] For example, the placement of functional groups at the termini or in well-defined segments can ultimately dictate their properties and provide highly controlled macromolecular systems.[14]

In the present work, we have used a third generation carbazole-terminated Fréchet-type polybenzylether dendrimers (G3-D), which have been synthesized in our group.[14,15] The concentration of the dendrimer was controlled in such a way that individual dendrimers are allowed to intramolecularly crosslink either chemically in solution or electrochemically at an interface. The crosslinking affects the size and rigidity of the electroactive dendrimer, which can be altered by controlling the extent of crosslinking of the peripheral carbazole groups using various polymerization methods. To our knowledge, this is one of the first attempts to produce intramolecularly crosslinked, conjugated dendrimers and investigate their nanoparticle properties. The crosslinking of the peripheral carbazole at the 3,6-positions leads to the formation of polycarbazole units.[16] In order to make the crosslinked dendrimer nanoparticles soluble and processable, precautions were made to avoid having any high degree of intermolecular crosslinking between the dendrimers. Thus, even after crosslinking, the dendrimer was found to be soluble in common organic solvents such as $CHCl_3$, CH_2Cl_2, tetrahydrofuran, and other polar solvents. The chemical crosslinking was performed using $FeCl_3$ as an oxidizing agent. The electrochemical crosslinking was also performed in situ using electrochemical nanolithography, in which the crosslinking occurs at the interface of an electrode substrate in a conducting atomic force microscopy (AFM) setup.

Firstly, the chemical crosslinking was performed using an ultradilute concentration (6.2×10^{-7} M) of the dendrimer G3-D in chloroform. The molar ratio of $FeCl_3$ to G3-D was set as 200:1.[16] At this dilution level, mostly intramolecular crosslinking occurs, i.e., formation of polycarbazole units at the surface of the dendrimer molecule, resulting in a crosslinked dendrimer (G3-D-CLK) as shown in Scheme 1. The extent of crosslinking was monitored using UV-vis spectroscopy. The G3-D shows an absorption peak at 325 nm and 345 nm, which are typically assigned to the π–π* and n–π* transitions of carbazole, respectively. After crosslinking, the π–π* transition is redshifted and observed as an adsorption tail extending into the visible range centered at 375 nm. This indicated the formation of higher π-conjugated species. The polymerization or crosslinking was performed until no further change was observed.

In addition to the electronic properties, one can utilize the fluorescent properties of polycarbazole to further confirm the crosslinking reaction. It was found that the dendrimer shows entirely different fluorescence spectra before and after crosslinking. The fluorescence of the carbazole units present on G3-D is observed at 360 nm (Figure 1B); this peak is

---

[*] Dr. R. Advincula, P. Taranekar, J.-Y. Park, D. Patton, T. Fulghum, G. J. Ramon
Department of Chemistry, University of Houston
136 Fleming Building, Houston, TX 77204-5003 (USA)
E-mail: radvincula@uh.edu

[**] The authors thank Prof. Eric Bittner for his assistance and helpful discussions. We gratefully acknowledge the partial funding from the Robert E. Welch Foundation (E-1551) and NSF DMR-0504435 and instrument support from DMR-0315565. We also acknowledge technical support from Molecular Imaging Inc. (Agilent Technologies). Supporting Information, including experimental and technical details involved in electrochemical crosslinking, self-assembled monolayer formation, and modeling calculations, is available online from Wiley InterScience or from the author.

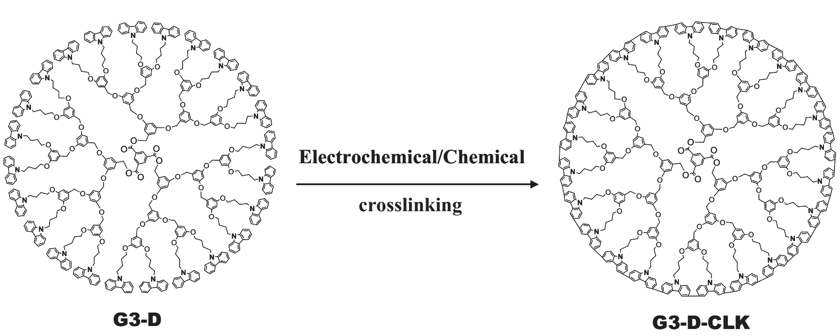

Scheme 1. Intramolecular crosslinking of peripheral carbazole to form polycarbazole. Note that the diagram is just a 2D representation of the crosslinking process.

quenched in the case of G3-D-CLK, where a new peak arises at 420 nm resulting from the formation of polycarbazole (inset, Figure 1B).

In order to further confirm the intramolecular crosslinking of the individual dendrimers based on a change in size, size exclusion chromatography (SEC) analysis was performed as shown in Figure 2A. A higher retention time was observed in going from G3-D (24.6 min) to G3-D-CLK (25.0 min), reflecting the more compact size of the crosslinked dendrimer, i.e., reduced hydrodynamic volume. In addition, at lower retention times the SEC elution curve of the G3-D-CLK also shows very small traces of dimer, trimer, or even higher analogs, which is evidence of some intermolecular crosslinking between dendrimer units. The extent of intramolecular crosslinking was also quantified using NMR spectroscopy. The integration of the peaks showed the extent of intramolecular crosslinking was more than 80 %. The protons at the 3- and 6-positions of the carbazole have a distinct signal at around $\delta = 8.01$ ppm that decreases upon crosslinking, indicating the formation of polycarbazole, as shown in Figure 2B. It

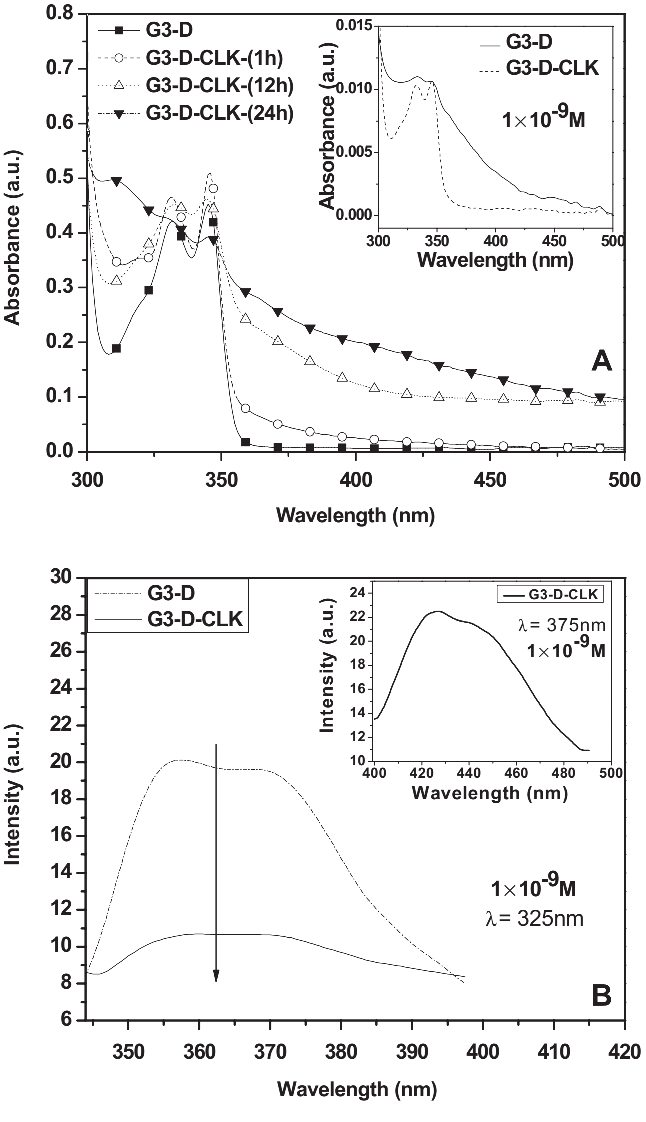

Figure 1. A) UV-vis spectra recorded at various intervals to monitor the extent of crosslinking, and inset showing a solution of 1×10^{-9} M G3-D dendrimer before and after crosslinking. Absorbance in absorbance units (a.u.). B) Fluorescence spectrum of G3-D at excitation of $\lambda = 325$ nm and inset showing the fluorescence spectrum G3-D-CLK (resulting from polycarbazole) after exciting at $\lambda = 375$ nm.

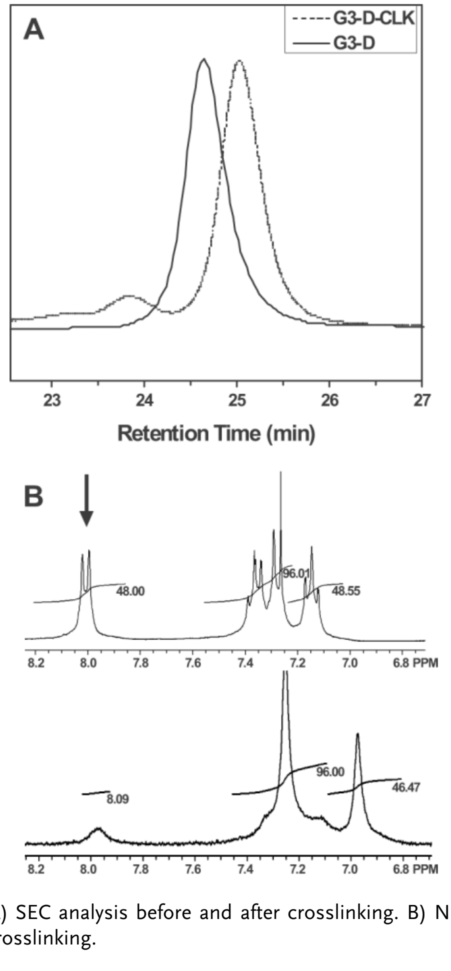

Figure 2. A) SEC analysis before and after crosslinking. B) NMR before and after crosslinking.

is highly unlikely to get complete intramolecular crosslinking within a dendrimer considering its 3D structure.

After crosslinking, both the crosslinked and uncrosslinked dendrimers were diluted to 1×10^{-12} M in chloroform and subsequently spin-coated (5000 rpm for 2 min) on atomically flat mica (freshly cleaved). AFM was performed using an acoustic mode (238.143 kHz, 1.49 lines s^{-1}) to visualize the distribution in size, shape, and rigidity of the dendrimer before and after crosslinking. However, the lateral size could not be determined due to convolution effects created by the AFM tip. Figure 3A shows a random distribution of the G3-D dendrimer nanoparticles and upon analysis of the statistical distribution, the height profile revealed the particle size to be 2.46 ± 0.24 nm. Figure 3D shows a high-resolution AFM image and the line profile of an individual uncrosslinked nanoparticle which was found to be 2.4 nm in height.

The G3-D dendrimer was found to lie more flat on the surface of mica. It is quite rational to observe this behavior because the uncrosslinked G3-D is more flexible in its structure. On the other hand, G3-D-CLK was found to have a higher statistical distribution in height (3.47 ± 0.23 nm) and a more compact shape, as shown in Figure 3B. Figure 3E shows a high-resolution AFM image and the line profile of an individual crosslinked dendrimer nanoparticles which was found to be 3.48 nm in height. Thus, the results show seemingly contradictory data in terms of change in height, while crosslinking results in the formation of a more rigid structure and a lower radius of gyration R_g value, owing to the compact nature of the crosslinked dendrimer.[12]

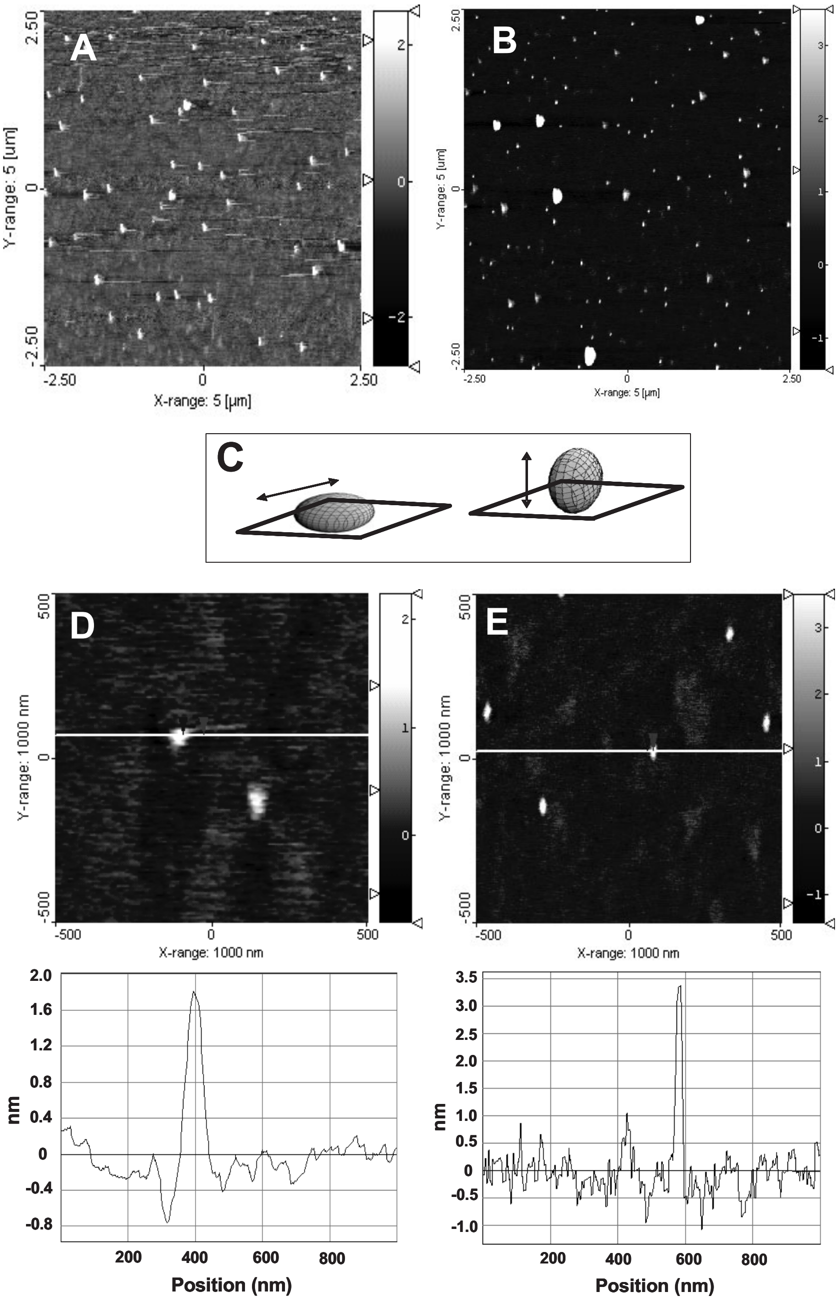

Figure 3. Tapping mode AFM pictures of A) G3-D (5 µm × 5µm) and B) G3-D-CLK (5 µm × 5µm). C) Model showing the effect of crosslinking (before (left) and after (right)). D) G3-D (1 µm × 1µm), E) G3-D-CLK (1 µm × 1µm).

To delineate the effect of rigidity and dendrimer nanoparticle–substrate interaction, we also studied the uncrosslinked and intramolecularly crosslinked dendrimer on a low free-energy silanized silicon wafer as compared to the high free-energy surface of mica. The dendrimers were spin-coated following similar protocols and using exactly the same solution concentrations as before. The sizes of these nanoparticles were found to be 2.7 nm and 3.6 nm for G3-D and G3-D-CLK, respectively. (Supporting Information, Figure S1) Clearly, there is a height difference of the dendrimer nanoparticles in going from one substrate to the other. Thus, for the case of G3-D on mica, a pancakelike conformation is seen, while G3-D-CLK adopts a more egglike conformation and remains unchanged in either case, as observed by AFM. In order to further probe the observed disparity in shape and size, we performed theoretical calculations aimed at understanding the structural changes of the dendrimers upon crosslinking. Figure 4 shows the optimized structures that were obtained using a molecular mechanics force-field implemented in Spartan'04 starting from an initial structure (Spartan'04, Wavefunction Inc. Irvine, CA, see Supporting Information).

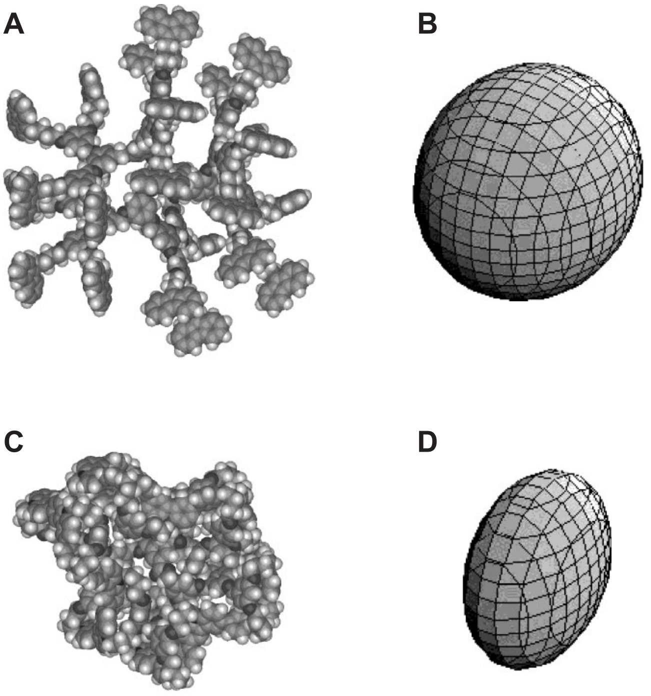

Figure 4. Energy optimized structures: A) Space filling representations of G3-D, B) expected shape of G3-D, C) space filling representations of G3-D-CLK, D) expected shape of G3-D-CLK. The decreased hydrodynamic volume is evident in the more compact structure after crosslinking.

The data, and the images in Figure 4B and D illustrate the shape of the dendrimer before and after crosslinking, and are generated from the final optimized structure. The shapes of the dendrimer were predicted by calculating the moment of inertia for the G3-D dendrimer before and after crosslinking. The moments of inertia were obtained by diagonalizing the moment of inertia tensor, I

$$I_{\mathrm{jk}} = \sum_{n} m_n \left(r_n^2 \delta_{\mathrm{jk}} - x_{n\mathrm{j}} x_{n\mathrm{k}} \right)$$

where x is the center of mass, m_n is the mass of the n^{th} atom (not the total mass), x corresponds to the (x,y,z) cartesian coordinates of the n^{th} atom relative to center of mass of the molecule, and r is the distance between atom i and the center of mass. (δ) corresponds to Kronecker delta; i, j, and k correspond to the Cartesian coordinates, and n corresponds to the index of the atom. I_{A}, I_{B}, and I_{C} are the components of the moment of inertia in the principal axis frame. Because $I_{\mathrm{A}} < I_{\mathrm{B}} \approx I_{\mathrm{C}}$ (conventionally $I_{\mathrm{C}} \geq I_{\mathrm{B}} \geq I_{\mathrm{A}}$) in each case, the molecules are roughly prolate-shaped ellipsoids. The fact that the G3-D has less disparity between I_{A} and $I_{\mathrm{B}} \approx I_{\mathrm{C}}$ than the G3-D-CLK case, indicates that the uncrosslinked molecule is less elongated (i.e., more spherical) than the crosslinked molecule as shown from I values in Table 1.

In order to compare and verify the height disparity observed in chemical crosslinking, we also attempted to study the in situ electrochemical crosslinking using the conducting-AFM method. In the past, we have demonstrated that the carbazole moiety can be electrochemically crosslinked using electrochemical nanolithography to form polycarbazole units, by using conducting AFM on a linear precursor polymer system.[17] Although the aim of this work is to investigate the effect of crosslinking on the size and rigidity of an individual dendrimer nanoparticles, the potential of local electrochemical manipulation at the nanometer scale can be extended to a range of applications such as the fabrication of conjugated molecular wires, optical microlenses, complex quantum devices, or tailored chemical surfaces for controlling biorecognition processes.[18] We have also previously investigated the electrochemical crosslinking of linear polycarbazole precursors in thin films to form conjugated polymer networks.[19]

Table 1. Moments of inertia for G3-D and G3-D-CLK dendrimers (amu: atomic mass unit).

Dendrimer	I_{A} [Å^2 amu]	I_{B} [Å^2 amu]	I_{C} [Å^2 amu]
G3-D-CLK	2.14×10^5	6.31×10^5	7.39×10^5
G3-D	0.779×10^6	1.08×10^6	1.15×10^6

An ultradilute solution of G3-D dendrimer (1×10^{-12} M) was again spin-coated on a gold (vacuum deposited on silicon wafer) substrate. Figure 5A shows a statistical distribution of the G3-D dendrimer particle size as 2.54 ± 0.19 nm along with some aggregates of dendrimers ranging from 15–21 nm. The average size of 2.54 nm of the G3-D dendrimer nanoparticles is very similar in size to the previous case on mica. The electrochemical crosslinking was performed by applying a voltage bias of –10 V in contact mode directly above the nanoparticles. The details of the conducting AFM setup and experimental conditions are described in the Supporting Information. The difference in the height is apparent as seen from Figure 5B, which shows a significant increase in height to about 3.82 ± 0.32 nm for most of the particles. We also found some particles in the size range of 4.2 nm. The variation in size was initially surprising, as one would expect to get a size range between 3 and 4 nm after crosslinking, as observed with the solution chemical crosslinking. It should be noted that these results are repeatable with variation of scan speed and that no crosslinking was observed below the –10 V bias.

Clearly, there is a difference in height and shape between the chemically crosslinked versus the electrochemically crosslinked dendrimer. One possibility is that in the process of applying a bias voltage, neighboring dendrimers can collectively crosslink intermolecularly, e.g., two closely located dendrimers can come together and crosslink to form a dimer. This is not unreasonable considering the size of the cantilever probe surface and the distribution of the electric field on the substrate (hundreds of nanometers). Another is the effect of humidity in the meniscus between the tip and the substrate and possible degradative oxidation with this method.[20] Yet another possibility is the combined effect of localized Joule heating and crosslinking.[21] However, more studies are needed using different experimental conditions in order to verify these possibilities.

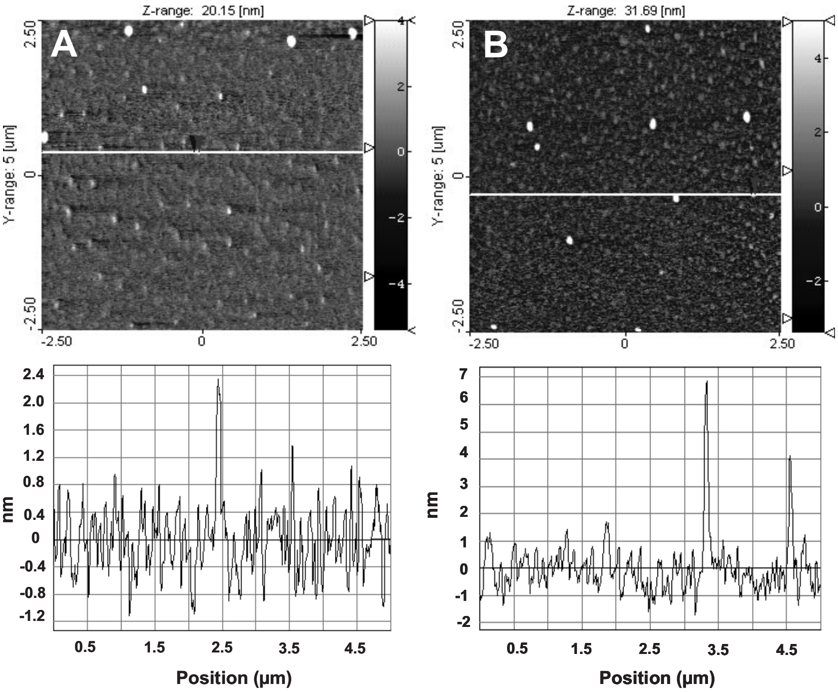

Figure 5. AFM images (5 µm × 5µm) of G3-D dendrimers A) before and B) after electrochemical crosslinking using tapping mode (topographical imaging) with a scan rate of 1.49 lines s^{-1}.

In conclusion, we have performed experimental and theoretical investigations of conjugated polymer nanoparticles brought upon by the intramolecular crosslinking of dendrimeric precursors using both chemical and in situ electrochemical methods. Both methods have shown variations in size and rigidity of the dendrimer nanoparticles, and regardless of crosslinking methods, the height of the crosslinked dendrimer was found to be higher than its uncrosslinked form. Finally, the models presented confirm both the size and rigidity of the organic nanoparticles, which can be fine-tuned by choosing the right conditions for either crosslinking method. Further studies are underway to investigate their current–voltage characteristics by current sensing AFM.

Received: March 8, 2006
Final version: June 29, 2006

---

[1] a) P. Furuta, J. Brooks, M. E. Thompson, J. M. J. Fréchet, *J. Am. Chem. Soc.* **2003**, *125*, 13 165. b) A. Adronov, J. M. J. Fréchet, *Chem. Commun.* **2000**, 1701. c) S. M. Grayson, J. M. J. Fréchet, *Chem. Rev.* **2001**, *101*, 3819. d) D. Ma, J. M. Lupton, R. Beavington, P. L. Burn, I. D. Samuel, *Adv. Funct. Mater.* **2002**, *12*, 507. e) J. S. Satoh, J.-S. Cho, M. Higuchi, K. Yamamoto, *J. Am. Chem. Soc.* **2003**, *125*, 8104.

[2] a) C. Devadoss, P. Bharathi, S. Moore, *J. Am. Chem. Soc.* **1996**, *118*, 9635. b) Y. Wang, M. I. Ranasinghe, T. Goodson, *J. Am. Chem. Soc.* **2003**, *125*, 9562.

[3] a) P. W. Wang, Y. J. Liu, C. Devadoss, P. Bharathi, J. S. Moore, *Adv. Mater.* **1996**, *8*, 237. b) J. M. Lupton, I. D. W. Samuel, R. Beavington, M. J. Frampton, P. L. Burn, H. Bassler, *Phys. Rev. B: Condens. Matter Mater. Phys.* **2001**, *63*, 155 206.

[4] a) J. S. Moore, *Acc. Chem. Res.* **1997**, *30*, 402. b) L. Gong, Q. Hu, L. Pu, *J. Org. Chem.* **2001**, *66*, 2358.

[5] A. J. Berresheim, M. Muller, K. Mullen, *Chem. Rev.* **1999**, *99*, 1747.

[6] a) C. Xia, X. Fan, J. Locklin, R. C. Advincula, *Org. Lett.* **2002**, *4*, 2067. b) C. Xia, X. Fan, J. Locklin, R. C. Advincula, A. Gies, W. Nonidez, *J. Am. Chem. Soc.* **2004**, *126*, 8735.

[7] a) A. Baba, K. Onishi, W. Knoll, R. C. Advincula, *J. Phys. Chem. B* **2004**, *108*, 18 949. b) H. J. Knolker, K. R. Reddy, *Chem. Rev.* **2002**, *102*, 4303. c) R. B. Kawde, K. S. V. Santhanam, *Bioelectrochem. Bioenerg.* **1995**, *38*, 405. d) D. Annie, J. E. Dubois, P. C. Lacaze, *J. Electroanal. Chem. Interfacial Electrochem.* **1985**, *189*, 51.

[8] a) A. Kimoto, J.-S. Cho, M. Higuchi, K. Yamamoto, *Macromolecules* **2004**, *37*, 5531. b) O. Varnavski, A. Leanov, L. Liu, J. Takacs, T. Goodson, III, *J. Phys. Chem. B* **2000**, *104*, 179.

[9] a) S. C. Zimmerman, M. S. Wendland, N. A. Rakow, I. Zharov, K. S. Suslick, *Nature* **2002**, *418*, 399. b) S. C. Zimmerman, I. Zharov, M. S. Wendland, N. A. Rakow, K. S. Suslick, *J. Am. Chem. Soc.* **2003**, *125*, 13 504.

[10] a) K. Emoto, M. Iijima, Y. Nagasaki, K. Kataoka, *J. Am. Chem. Soc.* **2000**, *122*, 2653. b) Y. Y. Won, H. T. Davis, F. S. Bates, *Science* **1999**, *283*, 960. c) F. Henselwood, G. Liu, *Macromolecules* **1997**, *30*, 488.

[11] a) T. Sanji, Y. Nakatsuka, S. Ohnishi, H. Sakurai, *Macromolecules* **2000**, *33*, 8524. b) J. F. Ding, G. J. Liu, *Macromolecules* **1998**, *31*, 6554. c) S. Stewart, G. J. Liu, *Chem. Mater.* **1999**, *11*, 1048. d) J. D. Hartgerink, E. Beniash, S. I. Stupp, *Science* **2001**, *294*, 1684.

[12] a) N. G. Lemcoff, T. A. Spurlin, A. A. Gewirth, S. C. Zimmerman, J. B. Beil, S. L. Elmer, H. G. Vandeveer, *J. Am. Chem. Soc.* **2004**, *126*, 11 420. b) S. L. Elmer, S. C. Zimmerman, *J. Org. Chem.* **2004**, *69*, 7363. c) J. B. Beil, N. G. Lemcoff, S. C. Zimmerman, *J. Am. Chem. Soc.* **2004**, *126*, 13 576.

[13] a) T. E. Dukette, M. E. Mackay, B. Van Horn, K. L. Wooley, E. Drockenmuller, M. Malkoch, C. J. Hawker, *Nano Lett.* **2005**, *5*, 1704. b) D. Benoit, V. Chaplinski, R. Braslau, C. J. Hawker, *J. Am. Chem. Soc.* **1999**, *121*, 3904.

[14] J. M. J. Fréchet, *Science* **1994**, *263*, 1710.

[15] Complete synthesis and characterization protocol: P. Taranekar, T. Fulghum, D. Patton, unpublished.

[16] D. B. Romero, M. Schaer, M. Leclerc, D. Ades, A. Siove, L. Zuppiroli, *Synth. Met.* **1996**, *80*, 271.

[17] S. Jegadesan, S. Sindhu, R. C. Advincula, S. Valiyaveettil, *Langmuir* **2006**, *22*, 780.

[18] a) J. R. Hampton, A. A. Dameron, P. S. Weiss, *J. Am. Chem. Soc.* **2006**, *128*, 1648. b) C. L. Cheung, J. A. Camarero, B. W. Woods, T. Lin, J. E. Johnson, J. J. De Yoreo, *J. Am. Chem. Soc.* **2003**, *125*, 6848. c) R. V. Martinez, R. Garcia, *Nano Lett.* **2005**, *5*, 1161. d) Y. Cai, B. M. Ocko, *J. Am. Chem. Soc.* **2005**, *127*, 16 287.

[19] a) A. Baba, K. Onishi, W. Knoll, R. C. Advincula, *J. Phys. Chem. B* **2004**, *108*, 18 949. b) P. Taranekar, A. Baba, T. M. Fulghum, R. Advincula, *Macromolecules* **2005**, *38*, 3679. c) S. Inaoka, D. B. Roitman, R. C. Advincula, *Chem. Mater.* **2005**, *17*, 6781.

[20] a) J. H. Lim, C. A. Mirkin, *Adv. Mater.* **2002**, *14*, 1474. b) R. D. Piner, C. A. Mirkin, *Langmuir* **1997**, *13*, 6864.

[21] a) S. F. Lyuksyutov, P. B. Paramonov, S. Juhl, R. A. Vaia, *Appl. Phys. Lett.* **2003**, *83*, 4405. b) S. Juhl, D. Phillips, R. A. Vaia, S. F. Lyuksyutov, P. B. Paramonov, *Appl. Phys. Lett.* **2004**, *85*, 3836. c) S. Jegadesan, R. C. Advincula, S. Valiyaveettil, *Adv. Mater.* **2005**, *17*, 1282. d) S. Jegadesan, P. Taranekar, S. Sindhu, R. C. Advincula, S. Valiyaveettil, *Langmuir* **2006**, *22*, 3807.